Science Arts & Métiers (SAM)

is an open access repository that collects the work of Arts et Métiers Institute of Technology researchers and makes it freely available over the web where possible.

This is an author-deposited version published in: https://sam.ensam.eu
Handle ID: .http://hdl.handle.net/10985/9801

To cite this version :

Thècle RIBERI-BÉRIDOT, Nathalie MANGELINCK-NOËL, Amina TANDJAOUI, Guillaume REINHART, Bernard BILLIA, Tamzin LAFFORD, José BARUCHEL, Laurent BARRALLIER - On the twinning impact on the grain structure formation of multi-crystalline silicon for photovoltaic applications during directional solidification - Journal of Crystal Growth n°418, p.38-44 - 2015

Any correspondence concerning this service should be sent to the repository Administrator : scienceouverte@ensam.eu

Arts et Métiers Institute of Technology

On the impact of twinning on the formation of the grain structure of multi-crystalline silicon for photovoltaic applications during directional solidification

Thècle Riberi-Béridot [a,*], Nathalie Mangelinck-Noël [a], Amina Tandjaoui [b], Guillaume Reinhart [a], Bernard Billia [a], Tamzin Lafford [c], José Baruchel [c], Laurent Barrallier [d]

[a] Aix-Marseille Université, CNRS, IM2NP UMR CNRS 7334, Campus Saint Jérôme, Case 142, 13397 Marseille Cedex 20, France
[b] Laboratoire de Mécanique de Lille (UMR CNRS 8107), Ecole Centrale de Lille, CS-20048, F-59651 Villeneuve d'Ascq Cedex, France
[c] ESRF, 71 avenue des Martyrs, CS40220, 38043 Grenoble Cedex 9, France
[d] Arts et Metiers ParisTech/Institut Carnot Arts Centre, Aix-en-Provence 2, cours des Arts et Métiers, 13617 Aix-en-Provence Cedex 1, France

Keywords:
A1. Directional solidification
A1. X-ray topography
A2. Growth from melt
B2. Semiconducting silicon
Electron Backscattered Diffraction
Grain competition

A B S T R A C T

Grain orientation and competition during growth has been analyzed in directionally solidified multi-crystalline silicon samples. *In situ* and real-time characterization of the evolution of the grain structure during growth has been performed using synchrotron X-ray imaging techniques (radiography and topography). In addition, Electron Backscattered Diffraction has been used to reveal the crystalline orientations of the grains and the twin relationships. New grains formed during growth have two main origins: random nucleation and twinning. It is demonstrated that the solidified samples are dominated by $\sum 3$ twin boundaries showing that twinning on {111} facets is the dominant phenomenon. Moreover, thanks to the *in situ* characterization of the growth, it is shown that twins nucleate on {111} facets located at the sides of the sample and at grain boundary grooves. The occurrence of multiple $\sum 3$ twins during growth prevents the initial grains from developing all along the sample, and twin boundaries with higher order coincidence site lattices can form at the encounter of two grains in twin position. The grain competition phenomenon following nucleation and twinning acts as a grain selection mechanism leading to the final grain structure.

1. Introduction

In the last few years, the evolution of the economic energy market has resulted in a considerable introduction of various renewable energies and technologies in daily life. The photovoltaic industry is one answer to the urgent need for renewable energies but faces competition from carbon and other renewable energies. In this context, recent work has focused on the improvement of multi-crystalline silicon (mc-Si) which presents an interesting €/Watt ratio in the production of photovoltaic panels [1,2]. However, mc-Si has an extremely heterogeneous grain structure that directly affects the solar cell efficiency *via* defects such as grits [3], grain boundaries, impurity segregation [4] and dislocations [5,6]. The knowledge of solidification mechanisms is essential and allows control of the final grain arrangement, the occurrence of structural defects and thus the final solar cell efficiency.

To unveil solidification mechanisms during silicon growth, an original directional solidification device was designed, enabling *in situ* and real-time characterization of the growth to be performed using synchrotron X-ray imaging techniques [7]. These techniques have been successfully used in previous studies to deepen the understanding of the grain formation mechanisms in mc-Si. Grain boundary groove dynamics have been studied and were found to play a significant role in grain selection and competition during growth [8] in agreement with existing theories [9]. The occurrence of twins has also been characterized [10].

However, a key issue remains, which is the relationship between the observed growth mechanisms, the grain orientation and the grain boundary type. Indeed, various studies show that the crystalline quality of the ingot and the twin relationship between the grain boundary types can have a significant impact on the photoelectric properties [11,12]. Moreover, although it has been shown that $\sum 3$ twins have no major impact on the photovoltaic properties, the repetition of twinning has important consequences for the final grain structure and distribution of crystallographic orientations [13,14]. The grain orientation and the grain boundary coincidence site lattice (CSL)

* Corresponding author.
E-mail address: thelce.riberi-beridot@im2np.fr (T. Riberi-Béridot).

have been previously studied in cast multi-crystalline silicon ingots by Electron Backscattered Diffraction (EBSD) [15,16]. In particular, the importance of twinning in the development of the grain structure has been highlighted for different solidification processes ranging from directional solidification [17] to ribbon growth [18].

In the present study, the grain structure formation in directionally solidified mc-Si samples has been characterized by correlating *post mortem* EBSD analyses with *in situ* X-ray imaging observations during growth, and the grain nucleation conditions as well as the grain competition during growth are discussed.

2. Experimental methodology

The directional solidification of thin mc-Si samples is carried out. The mc-Si samples from pure quality (6 N) are introduced in a high temperature furnace made of two resistive zones in a vacuum chamber. This experimental device is described in detail in [7,8,10]. The sample size is fixed at 5.6×38 mm^2 (length $\times$ width), and 300 μm in thickness. The experiments were performed at the ESRF (European Synchrotron Radiation Facility) on the BM05 beamline. Two X-ray imaging modes were used: X-ray radiography and X-ray topography (also called X-ray diffraction imaging). For both imaging modes, the solidifying sample was illuminated by a polychromatic (white) X-ray synchrotron beam (Fig. 1). To perform X-ray radiography (Fig. 1a), the beam was monochromated at 17.5 keV by a double Si(111) monochromator after crossing the sample and the images were recorded on a FReLoN CCD camera [19]. This allowed us to follow *in situ* and in real-time the evolution of the solid–liquid interface during growth with a large field of view (10 mm $\times$ 6 mm), sufficient spatial resolution (pixel size 7.46 μm $\times$ 7.46 μm) and temporal resolution (acquisition time 1 s). By this means, measurement of the solid–liquid interface growth velocity could be directly obtained.

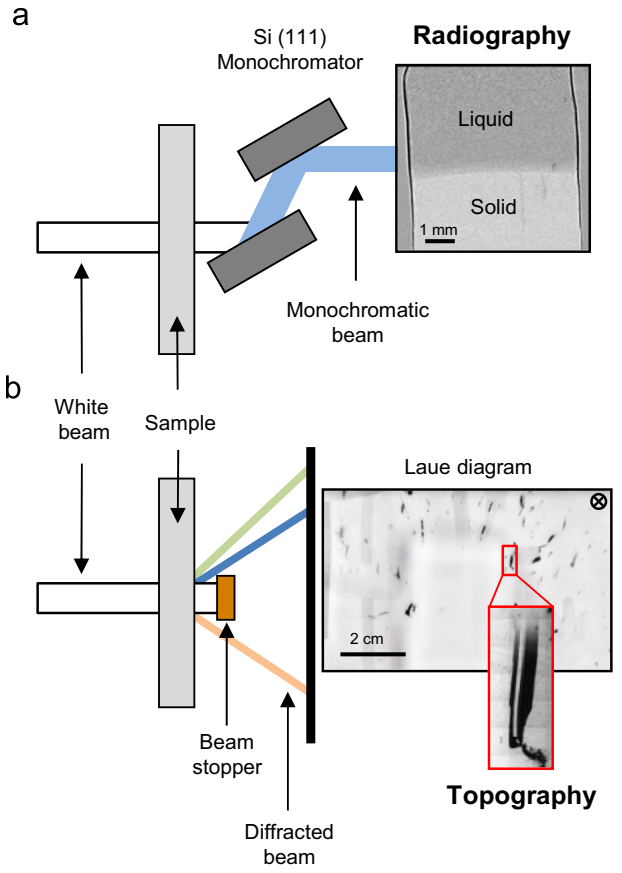

Fig. 1. Schematic illustration of synchrotron X-ray radiography and X-ray topography imaging techniques during directional solidification of a multi-crystalline silicon sample.

To perform X-ray topography (Fig. 1b), the white beam was stopped by a beam-stopper consisting in a small copper plate positioned near the furnace exit window. Beams were diffracted by the solid grains in the sample according to Bragg's law [19]. An X-ray sensitive film (AGFA Structurix D3-SC, 17.6×12.5 cm^2) was placed 30.6 cm from the sample and exposed to the diffracted beams. A Laue diagram was thus recorded and the diffraction spots were examined after the experiment with an optical microscope (Olympus BX51WI). Each spot is identified by its diffraction vector **g** and Miller indices. It is worth specifying that one grain has several diffraction spots with different intensities depending on the crystallographic orientation of its diffracting planes and the energy of the diffracted beam. Furthermore, large diffraction spots were obtained because the synchrotron beam width and height were selected to correspond to the size of the sample. The large diffraction spots (also called topographs) are images that contain information on the individual grain shape and deformation. Several films were successively exposed during solidification so that the evolution of the different grains could be followed. X-ray topographs provide useful information on the growth of isolated grains and on the occurrence of twinning because the image of a twin will appear at different positions in the Laue diagram, except when the Miller indices of the diffraction spot corresponds to those of the twinning plane. More information on these X-ray imaging modes and techniques can be found in [10].

Several melting/solidification cycles were carried out on each sample. Directional solidification was obtained by applying a constant positive temperature gradient G between the two heaters, and a cooling rate R to both heaters. After the last solidification, chemical etching using CP4 solution (18 ml HF+57 ml HNO3+25 ml CH3COOH) was performed to reveal the final grain structure of the samples. Finally, EBSD analysis was carried out in order to extract the three-dimensional orientation of each grain. The equipment used for this analysis was a JEOL JMS 6400 scanning electron microscope (SEM) coupled with an HKL EBSD camera, and the scanning step was 15 μm. Color grain orientation maps were generated with respect to the direction perpendicular to the sample surface and in the growth direction. Composite images of the etched sample and coincidence site lattice (CSL) order at the grain boundaries were also generated.

3. Results and discussion

In this part, we analyze EBSD and topography results obtained on two samples showing complementary growth and grain structure features. Fig. 2a shows an optical microscope image of the grain structure obtained after chemical etching of the first mc-Si sample. The temperature gradient applied was $G = 20 \pm 0.2$ K/cm. The solidification started after partial melting of the sample with an initial cooling rate of $R = 0.2 \pm 0.02$ K/min applied at a time t_0 for 20 min. After solidifying approximately 3 mm, the cooling rate was increased to 4 ± 0.02 K/min to finish the experiment. The measured growth rate was respectively 3.50 ± 0.03 μm/s and 22 ± 0.03 μm/s.

The corresponding EBSD results are given in Fig. 2b–d. Fig. 2b represents the coincidence site lattice (CSL) order of the grain boundaries. Fig. 2c and d are the crystalline grain orientation maps in the direction perpendicular to the sample surface and in the growth direction, respectively. Each color represents a crystallographic orientation according to the colored triangle next to Fig. 2d. It can be seen that grain 1, with a {101} plane parallel to the growth direction, started to grow from the initial seed and was able to develop across the field of view. Grain 2 nucleated on the right part

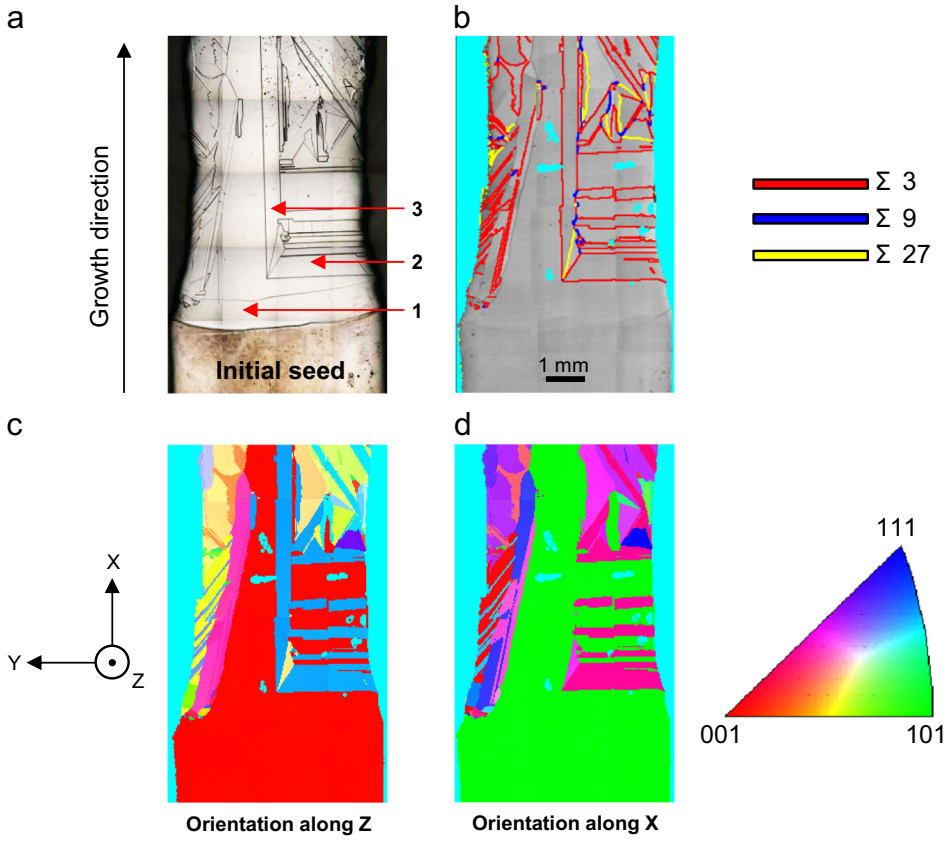

Fig. 2. (a) Optical microscope image showing the grain structure after chemical etching of a pure silicon sample (6 N) solidified with a cooling rate of $R=0.2$ K/min at t_0 and a cooling rate of $R=4$ K/min at t_0+20 min. The applied temperature gradient was $G=20$ K/cm. (b) Coincidence site lattice order of the grain boundaries (up to $\sum 27$). (c) Grain crystallographic orientation map in the *Z*-direction and (d) in the *X*-direction obtained by EBSD. (For interpretation of the references to color in this figure, the reader is referred to the web version of this article.)

of the sample with a different crystallographic orientation. Grain 2 is actually in twin relation with grain 1 according to Fig. 2b. Successive twinning occurred during its growth, characterized by the alternation of two crystallographic orientations (Fig. 2c–d). The width of twinned grain 2 does not change significantly during its growth until it is blocked by the random nucleation of grains above it following the increase in cooling rate. It can be noted that all twin boundaries of grain 2 are of $\sum 3$ type in the growth direction (Fig. 2b). This corresponds to twins that nucleated on {111} facets and that are due to a 60° (or equivalently 180°) rotation around the normal to the facet. It is worth noticing that the $\sum 3$ type grain boundaries dominate, at more than 75% in the whole sample. $\sum 9$ and $\sum 27$ types are also observed but do not exceed 5% and 6%, respectively. It is essential to note that these higher disordered twin boundaries appear mainly in two cases: at the encounter of two grains that previously nucleated with a $\sum 3$ type relationship from the same grain and at multiple nucleation events in the upper region due to the faster cooling rate. A good example of the former case is the encounter of grain 3, also holding a twin relation with grain 1, with the successive twins of grain 2 generating $\sum 9$ twin boundaries (Fig. 2b). It can also be noted that there is no growth competition between grains 1 and 3 whereas the growth of grain 1 was initially hindered by the growth of grain 2. This is due to the fact that grains 1 and 3 have the same crystallographic orientation in the growth direction. Their grain boundary is therefore parallel to the growth direction as previously reported by Tandjaoui et al. [8] and Duffar et al. [9].

Fig. 3 presents the optical image of the sample after solidification (Fig. 3a) and an image obtained from radiography by image processing to reveal the solid–liquid interface (Fig. 3b). More details about the image processing can be found in [10]. A grain boundary groove is visible at the solid–liquid interface in the close-up Fig. 3b. Fig. 3d–g shows close-ups of a diffraction spot with Miller indices $(\bar{1}\,\bar{1}\,2)$ collected at different instants during the solidification and corresponding to the twins of grain 2 in Fig. 2 and to the grain on the right side of Fig. 3b. More information on the development of this grain can be retrieved from the *in situ* and real-time observation of the topographs. It is worth noting that on topograph images the liquid is not observed because only the solid phase diffracts. The successive twins are immediately visible on these topographs from their striped appearance, which confirms that the crystals have the same crystallographic orientations after two successive twinning events. The upper part of the diffraction spots in Fig. 3d–f corresponds to the solid–liquid interface and the three upper twins are more developed in the growth direction on the right side. This triangular shape indicates that the nucleation of the twins occurred at the right hand side of the sample. After nucleation, the left side of the new grains had less time to develop in the growth direction because it first needed to grow from the right towards the center of the sample. This observation is in agreement with previous work [10] and confirms that twins do not nucleate uniformly on facets during successive twin growth. Many successive twins are also visible on the left side of the sample (Fig. 2). This can be explained by considering the fact that the sides of the sample where the liquid, the solid and the crucible meet during growth is a triple phase point where the heterogeneous nucleation of new grains is energetically favored [13].

Another experiment was selected to discuss complementary features related to the grain structure formation in mc-Si and is

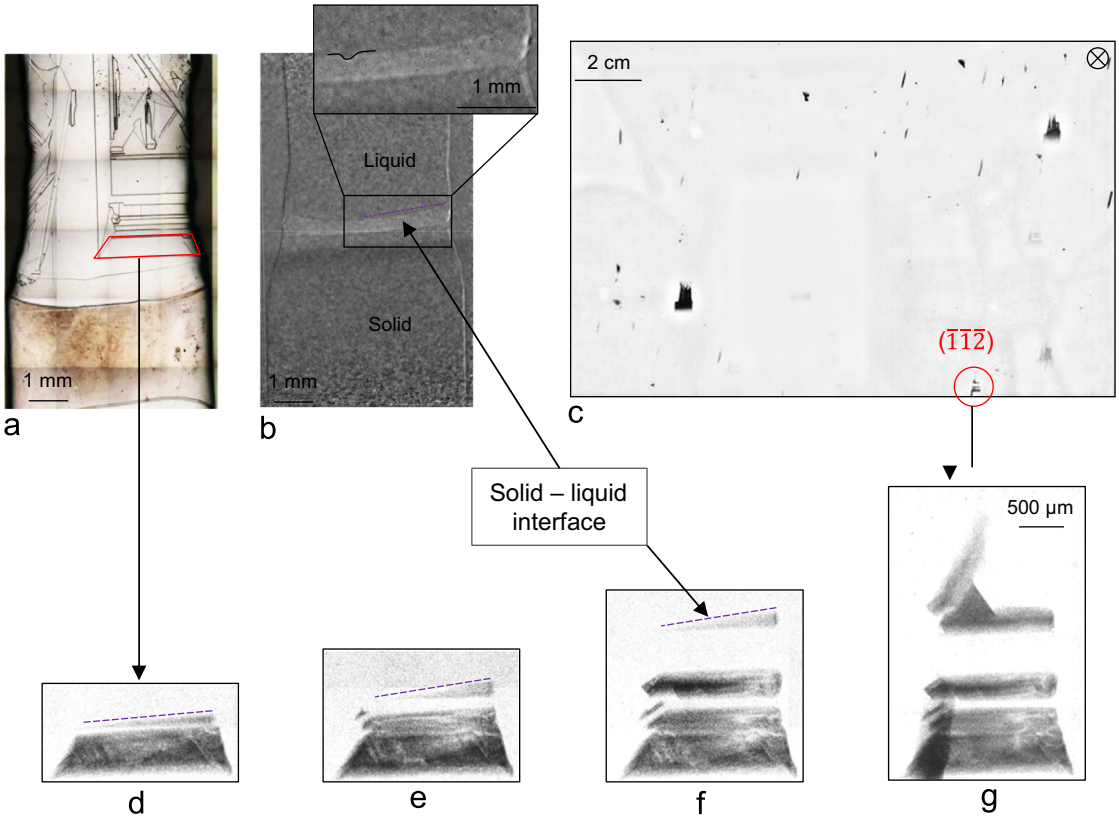

Fig. 3. (a) Optical microscope image showing the grain structure after chemical etching of a silicon sample (6 N) solidified with a cooling rate of $R=0.2$ K/min ($Vg=3.5$ µm/s) at t_0 and a cooling rate of $R=4$ K/min ($Vg=22$ µm/s) at t_0+20 min. The temperature gradient applied was $G=20$ K/cm. (b) Radiograph showing the solid–liquid interface at t_0+564 s, the close-up highlights the presence of a grain boundary groove. (c) Laue diagram recorded at t_0+1246 s. Close-ups of diffraction spots at (d) t_0+180 s; (e) t_0+420 s; (f) t_0+900 s; and (g) t_0+1246 s.

described in the following. In Fig. 4a, an optical microscope image of the grain structure of mc-Si sample of pure quality (6 N) is shown after solidification and after CP4 chemical etching. The grain structure obtained results from a solidification with a cooling rate of 2 ± 0.02 K/min applied to both heaters at t_0 from a partially melted sample. The initial temperature gradient was $G=15 \pm 0.2$ K/cm and the measured growth rate was 23 ± 0.03 µm/s.

The corresponding EBSD results are shown in Fig. 4b–d. Fig. 4b represents the coincidence site lattice (CSL) order of the grain boundaries. Fig. 4c and d are the crystalline grain orientation maps in the direction perpendicular to the sample surface and in the growth direction, respectively. Examination of these maps on Fig. 4c and d enables us to deepen our understanding of the phenomena occurring during growth while the grain structure is being established. In this experiment, twinned grain 7 nucleated on a {111} facet of grain 3. The multiple twins that nucleated during the growth of grain 7 are distinguished by the alternation between purple and red colors in Fig. 4d.

A grain competition mechanism is observed between grain 3 and grain 7. Twinned grain 7 grew to the detriment of grain 3 until the growth of the latter was finally stopped. The twinning of grain 7 with grain 3 led ultimately to a grain selection phenomenon. This grain competition is all the more rapid in this experiment as the {111} facet angle relatively to the growth direction is actually about 45°. This configuration should be avoided when one wants to grow ingots from a seed with a directional solidification process as for example in the mono-like growth method as shown in [18,20]. Moreover, grain 3 cannot extend on the right hand side since another grain has nucleated in the twin position (grain 8 in Fig. 4d).

Besides, it can be noticed that the presence of multiple twins did not disturb the growth of grain 7. In the same way, grain 1 nucleated on a facet in the gap left by grain 7 at the sides of the sample. Multiple twins nucleated also in grain 1 and easily extended in width. It is also interesting to observe the occurrence of grain 2 (Fig. 4d) which nucleated at the grain boundary groove formed at the encounter between grains 3 and 5. After nucleation, grain 2 entered into competition with grains 3 and 5 and was finally stopped by further grain nucleation.

An additional relevant point is the reproducibility in the grain boundary type proportion in comparison to the previous sample. In the present sample, twin boundaries are also dominant with $\sum 3$ grain boundaries in a proportion of more than 85%. It must be stressed that it is the case in all the samples we measured using EBSD after our experiments in spite of the different solidification conditions. In the work of Trempa et al. [20], they showed that grain boundaries in mono-like silicon ingots are mostly of $\sum 3$ type. Gallien et al. [15] and Voigt et al. [14] also studied the grain boundary type proportion in mc-Si cast wafers and they also observed that a majority of grain boundaries are twin grain boundaries. However, a higher proportion of high order CSL was obtained than in our results. In the study by Gallien et al. [15], $\sum 3$ grain boundaries did not exceed 48% and the maximum proportions observed of $\sum 9$ and $\sum 27$ were 15% and 6%, respectively. The solidification process in these experiments was different from our study since Gallien et al. studied ingots from cold crucible continuous casting, for which the solid–liquid interface is strongly convex because of the electromagnetic stirring [21] so that the growth direction varies along the interface. This has a high impact on grain competition and can explain the existence of many high CSL boundaries. In the case of Voigt et al. [14], mc-Si wafers of 5×5 cm^2 in dimension were grown by classical directional solidification. In comparison to this work, the main difference is our

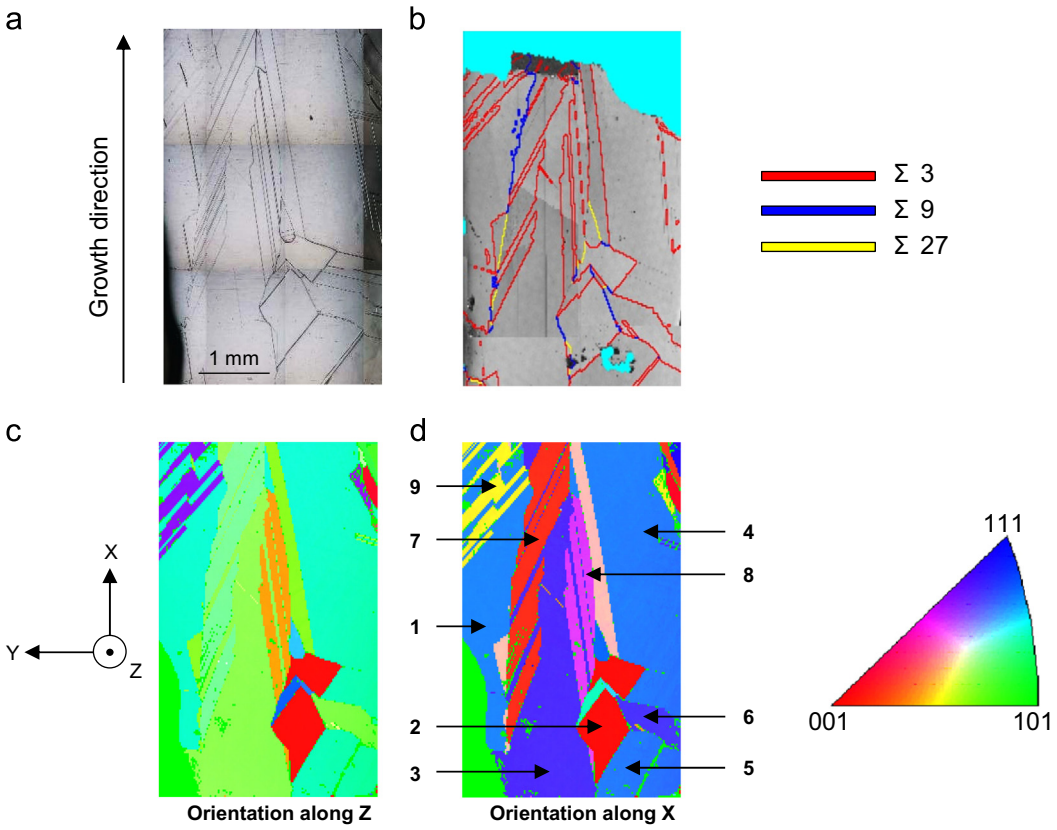

Fig. 4. (a) Optical microscope image showing the grain structure after chemical etching of a pure silicon sample (6 N) solidified with a cooling rate of $R=2$ K/min at t_0. The temperature gradient applied was $G=15$ K/cm and the measured growth rate was $Vg=23$ μm/s. (b) Coincidence site lattice order of the grain boundaries (up to $\sum 27$). (c) Grain crystallographic orientation map in the *Z*-direction and (d) in the *X*-direction obtained by EBSD. (For interpretation of the references to color in this figure, the reader is referred to the web version of this article.)

sample dimension (0.56×3.8 cm^2) that may have an impact on this result. In fact, it can be expected that for samples of higher volume and thus longer growth length, multiple $\sum 3$ twinning and the encounter of $\sum 3$ twins that have nucleated on different grains will yield a higher proportion of high CSL as previously describe in Fig. 2.

Another origin of higher order grain boundary type is the nucleation of a random grain. However, this is not the main mechanism observed in our experiments. The formation of higher order twin boundaries is mostly derived from an encounter of two twins of low order. This conclusion remains valid for most of processing parameters in our experiments.

Fig. 5 presents the EBSD orientation map along *X* direction after solidification (Fig. 5a) and an image obtained from radiography by image processing to reveal the solid–liquid interface (Fig. 5b). Several faceted grain boundary grooves are visible at the solid–liquid interface in the close-up Fig. 5b. Fig. 5d–i shows X-ray topographs that correspond to the same experiment. In Fig. 5d–f and Fig. 5g–i, the evolution of the spots noted A and B is shown, respectively. On spot A, grains 3 and 6 are identified. They are at the same diffraction position because they own the same crystallographic orientation, as can also be seen on the EBSD orientation map (Fig. 4). Moreover, multiple twins diffract also at this position and correspond to the areas colored in grain 7 (Fig. 4). In spot B, grains 1, 4 and 5 are identified and diffract at the same position because they have the same crystallographic orientation (Fig. 4). Indeed, it is important to stress the fact than in topographs, several grain images can be superimposed because grains have the same crystallographic orientation or a common plane corresponding to the given diffraction spot but at the same time can be far from each other in the sample (for example grains 1, 4 and 5 in Fig. 5i).

From the evolution of diffraction spot A (Fig. 5d–f) and from the CSL map (Fig. 4b), we learn that the twins in grain 7 nucleated at the level of a {111} facet but also that the nucleation was non-uniform. The onset of nucleation was on the left side, corresponding to the grain boundary groove between grains 1 and 7.

X-ray topography is highly sensitive to deformations of the crystallographic planes. Deformations are evidenced on the topographs by a distortion of the shape of the grain compared to the direct image in the radiograph or the metallograph. It is striking to note that the topographic images of grains containing multiple twins undergo no or only small deformation, whereas the topographic image of grain 4 that does not contain multiple twins is highly distorted. The physical origin of multiple twins in silicon is still under discussion in the literature [13]. However, one hypothesis is that multiple twins help to relax stresses during growth. A comparison of the behavior of grains that contain multiple twins with grains without twins could support this mechanism. Further investigations are still needed to completely unveil the twin nucleation mechanism.

4. Conclusion

This work contributes to unveiling the dynamics of the grain structure establishment mc-Si. Two characterization techniques have been used to understand the formation of the grain structure of mc-Si samples grown by directional solidification: X-ray topography, which enables us to follow *in situ* and in real time the grain formation; and EBSD analysis, which allows the relation between the crystallographic orientation of the grain and the observed growth phenomena to be established.

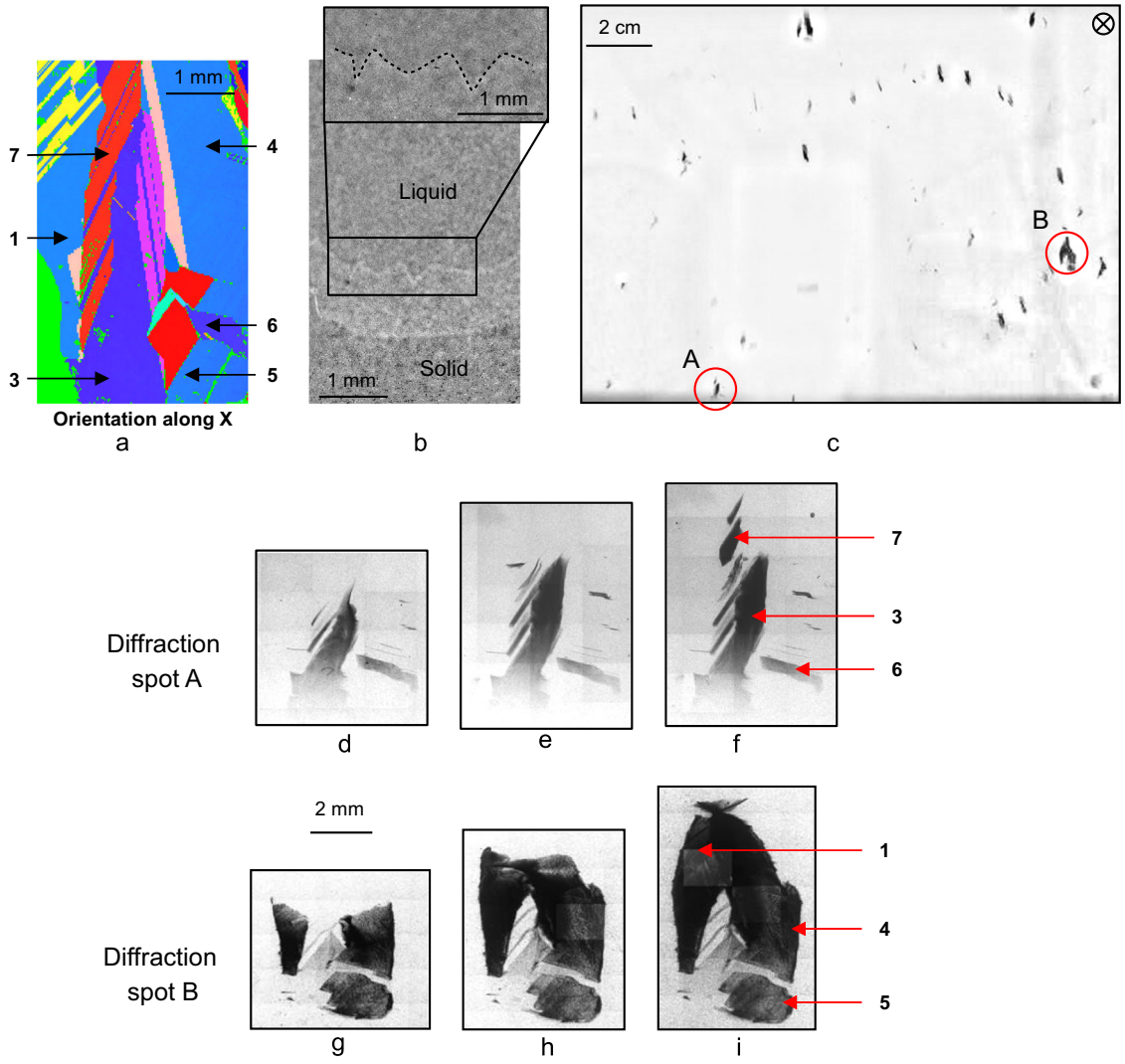

Fig. 5. (a) Grain crystallographic orientation map in the *X*-direction of a silicon sample (6 N) solidified with a cooling rate of $R=2$ K/min at t_0. The temperature gradient applied was $G=15$ K/cm and the measured growth rate was $Vg=23$ μm/s. (b) Laue diagram recorded at t_0+10 s. Close-ups of diffraction spots A and B at (c) and (f) t_0+8 min; (d) and (g) t_0+9 min; (e) and (h) t_0+10 min.

It was observed that twinning is the dominant mechanism for the formation of new grains during growth. Moreover, the majority of grain boundaries issue from ∑3 twins and few ∑9 and ∑27 boundaries were detected. Higher order twin boundaries were found to be due to two mechanisms: the encounter of two ∑3 twins or random nucleation, the former being the predominant mechanism. The major impact of ∑3 twin boundaries on the grain formation in multi-crystalline silicon was confirmed. As shown by several studies, these twins are considered not to be harmful to the photovoltaic properties of mc-Si [11]. However, it was observed in this work that they can be at the origin of the formation of higher order twin boundaries that are harmful for the PV properties and then cause disorder in grain structure.

Since they are the locus for all twin nucleation, {111} facets are essential features that have to be controlled since they are involved in the nucleation of parasitic grains and/or twins. Due to twinning, subsequent grain competition occurs, modifying drastically the initial or current grain arrangement and being able to prevent the growth of a selected crystallographic orientation. This is the topic of major recent studies [18,19] because this can cause the formation of parasitic grains when one wants to grow a mono-like silicon crystal from seed. Indeed, the presence of facets promotes nucleation of twins [22,23]. It has also been shown in the present experiments that facets promote the nucleation of twins when they are at the edge of the sample or at a grain boundary groove. As a consequence, it can be concluded that, to avoid parasitic nucleation and to control grain selection during growth, the occurrence of facets and their orientation relative to the growth direction should be controlled.

Considering the importance of twinning, further studies are needed to better understand their formation mechanisms and the involvement for mc-Si growth. Among other essential issues, twin nucleation related to strains or chemical reasons should be explored as well as the effects of the processing parameters and of the thermal field at the solid–liquid interface.

Acknowledgments

This work was part of the Si-X project funded by the (Grant no. ANR-08-HABISOL-012-01). The authors acknowledge the ESRF (European Synchrotron Radiation Facility) for beamtime allocation.

References

[1] I. Cerón, E. Caamaño-Martín, F.J. Neila, 'State-of-the-art' of building integrated photovoltaic products, Renew. Energy 58 (2013) 127–133.

[2] T.F. Ciszek, Photovoltaic materials and crystal growth research and development in the Gigawatt era, J. Cryst. Growth 393 (2014) 2–6.
[3] N. Mangelinck-Noël, T. Duffar, Modelling of the transition from a planar faceted front to equiaxed growth: application to photovoltaic polycrystalline silicon, J. Cryst. Growth 311 (1) (2008) 20–25.
[4] S. Martinuzzi, I. Périchaud, O. Palais, Segregation phenomena in large-size cast multicrystalline Si ingots, Sol. Energy Mater. Sol. Cells 91 (13) (2007) 1172–1175.
[5] N. Chen, S. Qiu, B. Liu, G. Du, G. Liu, W. Sun, An optical microscopy study of dislocations in multicrystalline silicon grown by directional solidification method (déc.), Mater. Sci. Semicond. Process. 13 (4) (2010) 276–280.
[6] E. Schmid, C. Funke, T. Behm, O. Pätzold, H. Berek, M. Stelter, Investigation of dislocation structures in ribbon- and ingot-grown multicrystalline silicon, J. Cryst. Growth 382 (2013) 41–46.
[7] A. Tandjaoui, N. Mangelinck-Noël, G. Reinhart, J.-J. Furter, B. Billia, T. Lafford, J. Baruchel, X. Guichard, Real time observation of the directional solidification of multicrystalline silicon: X-ray imaging characterization, Energy Procedia 27 (2012) 82–87.
[8] A. Tandjaoui, N. Mangelinck-Noel, G. Reinhart, B. Billia, T. Lafford, J. Baruchel, Investigation of grain boundary grooves at the solid–liquid interface during directional solidification of multi-crystalline silicon: *in situ* characterization by X-ray imaging, J. Cryst. Growth 377 (2013) 203–211.
[9] T. Duffar, A. Nadri, The grain–grain–liquid triple phase line during solidification of multi-crystalline silicon, C. R. Phys. 14 (2–3) (2013) 185–191.
[10] A. Tandjaoui, N. Mangelinck-Noel, G. Reinhart, B. Billia, X. Guichard, Twinning occurrence and grain competition in multi-crystalline silicon during solidification, C. R. Phys. 14 (2–3) (2013) 141–148.
[11] H.Y. Wang, N. Usami, K. Fujiwara, K. Kutsukake, K. Nakajima, Microstructures of Si multicrystals and their impact on minority carrier diffusion length, Acta Mater. 57 (11) (2009) 3268–3276.
[12] A. Autruffe, R. Søndenå, L. Vines, L. Arnberg, M. Di Sabatino, Influence of pulling rate on multicrystalline silicon ingots' properties, J. Cryst. Growth 386 (2014) 199–203.
[13] T. Duffar, Comprehensive review on grain and twin structures in bulk photovoltaic silicon, Recent Res. Dev. Cryst. Growth 5 (2010) 61–113.
[14] A. Voigt, E. Wolf, H.P. Strunk, Grain orientation and grain boundaries in cast multicrystalline silicon, Mater. Sci. Eng. B 54 (3) (1998) 202–206.
[15] B. Gallien, T. Duffar, S. Lay, F. Robaut, Analysis of grain orientation in cold crucible continuous casting of photovoltaic Si, J. Cryst. Growth 318 (1) (2011) 208–211.
[16] Y.T. Wong, C. Hsu, C.W. Lan, Development of grain structures of multi-crystalline silicon from randomly orientated seeds in directional solidification, J. Cryst. Growth 387 (2014) 10–15.
[17] C. Reimann, G. Müller, J. Friedrich, K. Lauer, A. Simonis, H. Wätzig, S. Krehan, R. Hartmann, A. Kruse, Systematic characterization of multi-crystalline silicon string ribbon wafer, J. Cryst. Growth 361 (2012) 38–43.
[18] A. Jouini, D. Ponthenier, H. Lignier, N. Enjalbert, B. Marie, B. Drevet, E. Pihan, C. Cayron, T. Lafford, D. Camel, Improved multicrystalline silicon ingot crystal quality through seed growth for high efficiency solar cells: improved mc-Si ingot crystal quality through seed growth, Prog. Photovolt. Res. Appl. 20 (6) (2012) 735–746.
[19] J.-C. Labiche, O. Mathon, S. Pascarelli, M.A. Newton, G.G. Ferre, C. Curfs, G. Vaughan, A. Homs, D.F. Carreiras, Invited article: the fast readout low noise camera as a versatile x-ray detector for time resolved dispersive extended X-ray absorption fine structure and diffraction studies of dynamic problems in materials science, chemistry, and catalysis, Rev. Sci. Instrum. 78 (9) (2007) 091301.
[20] M. Trempa, C. Reimann, J. Friedrich, G. Müller, D. Oriwol, Mono-crystalline growth in directional solidification of silicon with different orientation and splitting of seed crystals, J. Cryst. Growth 351 (1) (2012) 131–140.
[21] T. Liu, Z. Dong, Y. Zhao, J. Wang, T. Chen, H. Xie, J. Li, H. Ni, D. Huo, Purification of metallurgical silicon through directional solidification in a large cold crucible, J. Cryst. Growth 355 (1) (2012) 145–150.
[22] T. Duffar, A. Nadri, On the twinning occurrence in bulk semiconductor crystal growth, Scr. Mater. 62 (12) (2010) 955–960.
[23] D.T.J. Hurle, P. Rudolph, A brief history of defect formation, segregation, faceting, and twinning in melt-grown semiconductors, J. Cryst. Growth 264 (4) (2004) 550–564.